QCD phase diagram at finite baryon and isospin chemical potentials in the Polyakov loop extended quark meson model with vector interaction

H. Ueda,[1,2] T. Z. Nakano,[1,2] A. Ohnishi,[2] M. Ruggieri,[3] and K. Sumiyoshi[4]

[1]*Department of Physics, Faculty of Science, Kyoto University, Kyoto 606-8502, Japan*
[2]*Yukawa Institute for Theoretical Physics, Kyoto University, Kyoto 606-8502, Japan*
[3]*Department of Physics and Astronomy, University of Catania, Via S. Sofia 64, I-95125 Catania, Italy*
[4]*Numazu College of Technology, Ooka 3600, Numazu, Shizuoka 410-8501, Japan*

(Received 21 May 2013; published 8 October 2013)

We investigate the QCD phase diagram of isospin asymmetric matter using the Polyakov loop extended quark meson model with vector interaction. The critical point temperature is found to decrease in isospin asymmetric matter and disappear at large isospin chemical potential. We also discuss the QCD phase transition in the neutron star core. From comparison of the QCD phase diagram in Polyakov loop extended quark meson model and corresponding baryon and isospin chemical potentials of neutron star matter in relativistic mean-field models, we show that the order of the chiral phase transition in the neutron star core could be crossover because of large isospin chemical potential.

DOI: 10.1103/PhysRevD.88.074006 PACS numbers: 12.38.Lg, 21.65.Qr

I. INTRODUCTION

The QCD phase transition would be realized not only in heavy-ion collisions but also in compact astrophysical objects and phenomena such as heavy neutron stars [1], supernovae [2], and black hole (BH) formations [3–6]. At zero baryon chemical potential (μ_B), the QCD phase transition at finite temperature (T) is accessible by using the lattice Monte Carlo simulation, e.g., [7,8]. At large μ_B, $\mu_B/T \gtrsim 1$, the situation is much less clear, since the lattice simulation is plagued by the well-known sign problem [9]. We can investigate this region by using chiral effective models such as the Nambu–Jona-Lasinio (NJL) model [10] and the quark meson (QM) model [11], and those with the Polyakov loop effects such as the Polyakov loop extended Nambu–Jona-Lasinio (PNJL) model [12–14] and the Polyakov loop extended quark meson (PQM) model [15,16]. The QCD phase diagram, especially the QCD critical point (CP) location, strongly depends on models and model parameters [17]. Therefore, further experimental and theoretical developments are necessary to determine the structure of the QCD phase diagram.

For laboratory experiments, the search for CP in heavy-ion collisions is ongoing at RHIC [18] and is planned in the coming FAIR facility. Since the phase transition is second order at CP, the coherence length ξ is divergent, and large fluctuations of the order parameter are expected in a volume of the size ξ^3. Various signatures of CP have been proposed theoretically [19]. It is not an easy task to observe the divergence signature of ξ in heavy-ion collisions, since the system size and the evolution time are limited. Moreover, it is difficult to create cold dense matter, and CP may not be reachable in the laboratory if CP is located in the high-density region, $\mu_B > 500$ MeV.

By comparison, very dense matter is formed in compact astrophysical phenomena. For example, high-density and low-temperature matter is formed in the neutron star core, and high-temperature and high-density matter is produced during a gravitational collapse of a massive star and binary stars [20]. From the observation of these phenomena, we may get information on the QCD phase diagram in the high-density region [1–6]. In compact astrophysical phenomena, charge neutrality leads to suppressed proton fraction compared with that of neutrons, and the isospin chemical potential $\delta\mu \equiv (\mu_n - \mu_p)/2 = (\mu_d - \mu_u)/2$ is finite and positive. In particular, $\delta\mu$ appears as another independent thermodynamical variable in supernovae and BH formations, since trapped neutrinos modify the neutrinoless charge neutrality condition ($\delta\mu = \mu_e/2$). Therefore, it is necessary to consider $\delta\mu$ dependence of the QCD phase diagram in order to discuss the QCD phase transition in compact star phenomena.

The phase structure in the three thermodynamic variables (T, μ, $\delta\mu$) is still an open problem. In our previous work [6], we have discussed the possibility of the CP sweep during BH formation processes where $\delta\mu$ is finite; quark matter core and hadronic envelope may merge to one phase, when the temperature exceeds the CP temperature (T_{CP}). The location of CP strongly depends on $\delta\mu$; for large $\delta\mu$, T_{CP} becomes lower and it becomes more probable for the heated matter to go through CP. There are several recent works that discuss the QCD phase diagram in charge-neutral dense matter [21] and in the three-dimensional space, (T, μ, $\delta\mu$) [22,23] or (T, μ, μ_L) [24], where μ_L is the lepton-number chemical potential. The phase diagram structures in these works have some differences. In Ref. [21], the isospin chemical potential is found to be small $\delta\mu < m_\pi/2$, and pions are not found to condense in charge-neutral quark matter in the mean-field treatment of PNJL. In Ref. [22], three-dimensional (T, μ, $\delta\mu$) phase diagram is investigated in the mean-field approximation of PNJL, and the s-wave pion-condensed

phase is found to appear in the finite μ and $\delta\mu$ region. $T_{\rm CP}$ decreases with increasing $\delta\mu$ until the CP hits the pion condensation phase boundary. In Ref. [23], fluctuation effects are taken into account by using the functional renormalization group flow equation starting from the QM model as the initial condition at a large cutoff. $T_{\rm CP}$ is also found to decrease with increasing $\delta\mu$. The s-wave pion-condensed phase is found in the high-$\delta\mu$ and low-μ region, but it is suppressed at large μ. As a result, the pion-condensed phase is separated from the chiral first-order phase transition surface in the $(T, \mu, \delta\mu)$ space. In Ref. [24], $T_{\rm CP}$ is found to be insensitive to the lepton-number chemical potential in the mean-field treatment of PNJL.

In this paper, we investigate the isospin chemical potential dependence of the QCD phase diagram in more detail and discuss the order of the chiral phase transition in the neutron star core, where $T = 0$ and μ_B, $\delta\mu > 0$. For this purpose, we first compute the QCD phase diagram using the two-flavor PQM with vector interaction and examine the $\delta\mu$ dependence of the QCD phase diagram. According to the s-wave πN repulsion argument [25] and functional renormalization group results [23], we assume that pions do not condensate. We then discuss the order of the chiral phase transition in neutron star core. We obtain the β equilibrium line in neutron star matter in PQM. We also compare the QCD phase diagram with the β equilibrium line calculated by using the hadronic equations of state, where the nuclear matter saturation effects are respected.

The paper is organized as follows: In Sec. II, we briefly describe PQM with vector interaction. The results are discussed in Sec. III, where we show the $\delta\mu$ dependence of the QCD phase diagram and compare the QCD phase diagram in PQM with neutron star matter chemical potentials. Section IV is devoted to summary and discussion.

II. POLYAKOV LOOP EXTENDED QUARK MESON MODEL

A. PQM Lagrangian and parameters

In this section, we describe the PQM model augmented with the vector interaction. PQM is an effective model that has the chiral symmetry and confinement property of QCD [15,16]. The Lagrangian density of the two-flavor PQM is given by [15,16]

$$\begin{aligned}\mathcal{L} = {} & \bar{q}[i\gamma^\mu D_\mu - g(\sigma + i\gamma_5 \boldsymbol{\tau}\cdot\boldsymbol{\pi}) - g_\omega \gamma^\mu \omega_\mu \\ & - g_\rho \gamma^\mu \boldsymbol{\tau}\cdot\boldsymbol{R}_\mu]q + \frac{1}{2}(\partial_\mu\sigma)^2 + \frac{1}{2}(\partial_\mu\boldsymbol{\pi})^2 - U(\sigma,\boldsymbol{\pi}) \\ & - \frac{1}{4}\omega_{\mu\nu}\omega^{\mu\nu} - \frac{1}{4}\boldsymbol{R}_{\mu\nu}\cdot\boldsymbol{R}^{\mu\nu} \\ & + \frac{1}{2}m_v^2(\omega_\mu\omega^\mu + \boldsymbol{R}_\mu\cdot\boldsymbol{R}^\mu) - \mathcal{U}(P,\bar{P},T), \end{aligned} \tag{1}$$

where q denotes a quark field with Dirac, color, and flavor indices, $\boldsymbol{\tau}$ is the Pauli matrix in the flavor space, and $\omega^{\mu\nu}$ and $\boldsymbol{R}^{\mu\nu}$ are the field tensors of ω and ρ mesons. The mesonic potential U and the Polyakov loop potential $\mathcal{U}$ are given as

$$U(\sigma,\boldsymbol{\pi}) = \lambda(\sigma^2 + \boldsymbol{\pi}^2 - v^2)^2/4 - h\sigma, \tag{2}$$

$$\mathcal{U}[P,\bar{P},T] = T^4\left\{-\frac{a(T)}{2}\bar{P}P + b(T)\ln H(P,\bar{P})\right\}, \tag{3}$$

$$H(P,\bar{P}) = 1 - 6\bar{P}P + 4(\bar{P}^3 + P^3) - 3(\bar{P}P)^2, \tag{4}$$

where σ and $\boldsymbol{\pi}$ are the isoscalar-scalar and isovector-pseudoscalar meson fields. The covariant derivative $D_\mu = \partial_\mu - iA_\mu$ in Eq. (1) is the Dirac operator with a temporal static and homogeneous background gluon field $A_\mu = \delta_{\mu 0}A_0$. Without the explicit symmetry-breaking term, the last term in Eq. (2), the Lagrangian in Eq. (1) has $SU(2)_L \times SU(2)_R$ symmetry.

$\mathcal{U}(P,\bar{P},T)$ is an effective potential of the gluon field, where P and $\bar{P}$ are the Polyakov loop and its conjugate,

$$P = \frac{1}{N_c}\,\mathrm{Tr}L, \qquad \bar{P} = \frac{1}{N_c}\,\mathrm{Tr}L^\dagger. \tag{5}$$

L is defined in the Euclidean space as

$$L = \mathcal{P}\exp\left(i\int_0^\beta d\tau A_4\right), \tag{6}$$

where $\mathcal{P}$ stands for the path ordering. The logarithmic term $\ln H(P,\bar{P})$ in Eq. (3) comes from the Haar measure of the group integral in strong-coupling lattice QCD [13]. Coefficients $a(T)$ and $b(T)$ are given as functions of T, and parametrized as $a(T) = a_0 + a_1(T_0/T) + a_2(T_0/T)^2$ and $b(T) = b_3(T_0/T)^3$ [14].

B. Effective potential

We now give the effective potential in dense asymmetric matter in PQM. In asymmetric matter, u and d quark populations are unbalanced, and we need to introduce two independent chemical potentials for u and d quarks,

$$\mu_u = \mu - \delta\mu, \qquad \mu_d = \mu + \delta\mu, \tag{7}$$

where $\mu = \mu_B/3$ is the quark chemical potential. The isospin chemical potential $\delta\mu$ is an independent thermodynamical variable in supernovae or BH formation processes, while the neutrinoless β equilibrium condition, $\delta\mu = \mu_e/2$, applies to cold neutron star matter.

We assume that the σ meson and the temporal components of ω and ρ^0 mesons take finite expectation values, while others do not. These expected values are assumed to be constant. In this approximation, the quark single-quasiparticle energy is given by

$$E^*_{fp} = E_p + g_\omega\omega + g_\rho\tau^3 R, \tag{8}$$

with

$$E_p = \sqrt{\boldsymbol{p}^2 + M^2}, \qquad M = g\sigma. \tag{9}$$

ω and R in Eq. (8) denote the expectation values of ω and ρ^0 mesons ($\omega = \langle\omega_0\rangle$, $R = \langle R_0^3\rangle$), respectively, where the subscript 0 denotes the temporal component, and the superscript for R shows isospin. The effect of vector interaction is to shift the quark chemical potential [26]. For later convenience, we define effective chemical potentials for u and d quarks,

$$\begin{aligned}\tilde{\mu}_u &= \mu - \delta\mu - g_\omega\omega - g_\rho R,\\ \tilde{\mu}_d &= \mu + \delta\mu - g_\omega\omega + g_\rho R.\end{aligned} \tag{10}$$

Integrating over the quark fields results in the following effective potential,

$$\Omega_{\mathrm{PQM}} = \mathcal{U}(P, \bar{P}, T) + U(\sigma, \boldsymbol{\pi} = 0) + \Omega_0 + \Omega_T, \tag{11}$$

$$\Omega_0 = -2N_f N_c \int \frac{d\boldsymbol{p}}{(2\pi)^3} E_p \theta(\Lambda^2 - \boldsymbol{p}^2), \tag{12}$$

$$\begin{aligned}\Omega_T = &-\frac{1}{2}(m_\omega^2\omega^2 + m_\rho^2 R^2)\\ &- 2T\sum_f \int \frac{d\boldsymbol{p}}{(2\pi)^3} \log\left(F_-^f F_+^f\right),\end{aligned} \tag{13}$$

$$F_-^f = 1 + 3Pe^{-\beta\mathcal{E}_-^f} + 3\bar{P}e^{-2\beta\mathcal{E}_-^f} + e^{-3\beta\mathcal{E}_-^f}, \tag{14}$$

$$F_+^f = 1 + 3\bar{P}e^{-\beta\mathcal{E}_+^f} + 3Pe^{-2\beta\mathcal{E}_+^f} + e^{-3\beta\mathcal{E}_+^f}, \tag{15}$$

$$\mathcal{E}_\pm^f = E_p \pm \tilde{\mu}_f, \tag{16}$$

where Ω_T is the thermal contribution and Ω_0 is the fermion vacuum energy, regularized by the ultraviolet cutoff Λ. This term is necessary to reproduce the second-order chiral phase transition at zero baryon chemical potential μ_B in the chiral limit [16]. Each term on the right-hand side of Eq. (14) corresponds to the thermal contribution of zero, one, two, and three quark states. Similarly, Eq. (15) is the thermal contribution of antiquarks. While PQM is renormalizable and we can use dimensional renormalization [16], it is sufficient to cut large momenta by a hard cutoff for our purposes.

The equations of motion are obtained from the stationary conditions in equilibrium,

$$\frac{\partial\Omega}{\partial\sigma} = \frac{\partial\Omega}{\partial P} = \frac{\partial\Omega}{\partial\bar{P}} = \frac{\partial\Omega}{\partial\omega} = \frac{\partial\Omega}{\partial R} = 0. \tag{17}$$

We obtain (T, μ_B, $\delta\mu$) dependence of the mean fields, σ, P, $\bar{P}$, ω and R, by solving these equations.

C. Model parametrization

The parameters in the scalar-pseudoscalar part, g, λ, ν, h are fixed to reproduce some properties of quarks and mesons in vacuum for a given value of the hard momentum cutoff $\Lambda = 600$ MeV in this work. The quark-scalar meson coupling g is determined by the constituent quark mass in the vacuum $m_q = g\sigma = 335$ MeV. The mesonic potential parameters λ and υ are given by the chiral condensate in the vacuum $\sigma = f_\pi = 92.4$ MeV, and the σ meson mass $m_\sigma^2 = \partial^2\Omega/\partial\sigma^2 = (700\ \mathrm{MeV})^2$. The explicit symmetry-breaking parameter h is given by the pion mass $h = m_\pi^2 f_\pi$.

In this study, we assume the quark-vector couplings are the same ($g_\omega = g_\rho = g_\upsilon$) for simplicity. We regard g_υ as a free parameter, and we compare the results with several values of $r = g_\upsilon/g$. We also assume the common vector meson masses ($m_\omega = m_\rho = m_\upsilon = 770$ MeV).

The parameters in the Polyakov loop potential are fitted to the pure gauge lattice data [27]. The standard choice of the parameters reads [14] $a_0 = 3.51$, $a_1 = -2.47$, $a_2 = 15.2$ and $b_3 = -1.75$. The parameter T_0 in Eq. (3) sets the deconfinement scale in the pure gauge theory, i.e., $T_0 = 270$ MeV. Chemical potential dependence of these parameters is not considered in this work [15,28].

III. RESULTS

A. Phase diagram of asymmetric matter

In this section, we discuss the $\delta\mu$ and the vector coupling dependence of the QCD phase diagram. The chiral phase transition is found to be weakened at finite $\delta\mu$ or with finite vector coupling r. In order to demonstrate this point, we first discuss the order parameters as functions of μ_B at several values of $\delta\mu$ and r.

The phase structure is obtained from the behavior of the order parameters σ, P and $\bar{P}$. Figure 1 shows μ_B dependence of the order parameters, σ (left) and P (right), for several isospin chemical potentials at $T = 96.5$ MeV $= T_{\mathrm{CP}}(\delta\mu = 50\ \mathrm{MeV}, r = 0)$ (CP temperature at $\delta\mu = 50$ MeV and the vector-scalar coupling ratio $r = 0$). For small $\delta\mu$, the chiral phase transition is first order, while for $\delta\mu \gtrsim 50$ MeV, the chiral phase transition becomes crossover. The change of the nature of the phase transition with the increase of $\delta\mu$ is not a peculiarity of the PQM model; in fact, several chiral models share this property, as discussed in [6] (see also the Appendix for a discussion within the NJL model).

In Fig. 2, we show σ (left) and P (right) as functions of the baryon chemical potential at $T = 101.5$ MeV $= T_{\mathrm{CP}}(\delta\mu = 0, r = 0.2)$ and $\delta\mu = 0$ MeV for several values of the vector-scalar coupling ratio r. For the strong vector interaction, the transition chemical potential is shifted to higher values, and the chiral phase transition is smoothed. The transition becomes crossover for $r \gtrsim 0.2$ at this T.

We next discuss the $\delta\mu$ and vector coupling dependence of the chiral and deconfinement phase boundaries. Since the chiral phase transition at small μ_B is actually a smooth crossover for finite quark masses, we have to establish a criterion to identify the phase boundary of the chiral

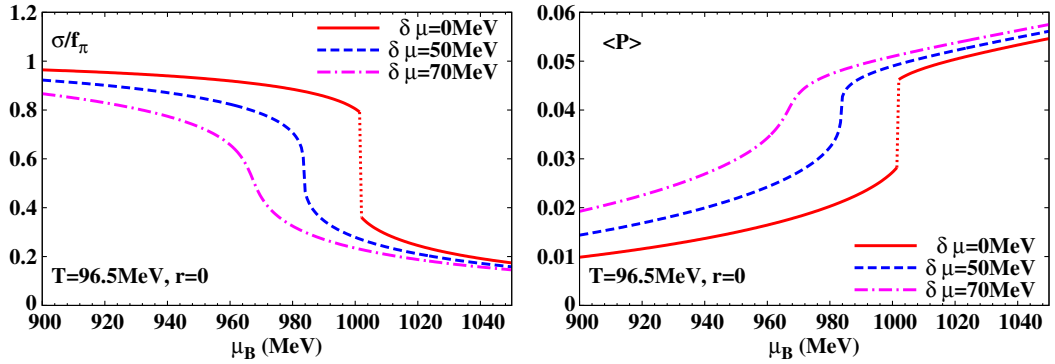

FIG. 1 (color online). The order parameters σ (left panel), P (right panel) as functions of baryon chemical potential μ_B at $T = 96.5$ MeV $= T_{\rm CP}(\delta\mu = 50$ MeV, $r = 0)$ and three different isospin chemical potentials $\delta\mu = 0$ (solid line), 50 (dash line), 70 MeV (dash-dot line). The vector-scalar coupling ratio is chosen to be $r = 0$.

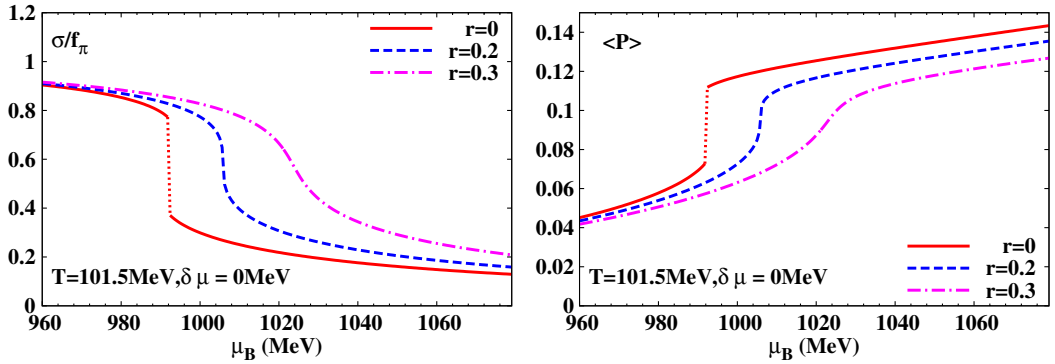

FIG. 2 (color online). The order parameters σ (left panel), P (right panel) as functions of baryon chemical potential μ_B at $T = 101.5$ MeV $= T_{\rm CP}(\delta\mu = 0$ MeV, $r = 0.2)$ and $\delta\mu = 0$ MeV for several values of the vector-scalar coupling ratio $r = 0$, 0.2, 0.3.

transition. Here we define the chiral critical temperature T_c or the baryon chemical potential $\mu_{B,c}$ of the chiral phase transition by the peak of the chiral susceptibility χ_σ as a function of T or μ_B for fixed $\delta\mu$ and μ_B or T, respectively. Since χ_σ is divergent at the critical point, we can unambiguously determine the critical point temperature $T_{\rm CP}$ and baryon chemical potential $\mu_{\rm CP}$ by the diverging peak of χ_σ in the $T - \mu_B$ plane. The chiral susceptibility is defined as the second derivative of the effective potential by the explicit chiral breaking coefficient h,

$$\chi_\sigma = -T^3 \frac{\partial^2(\Omega/T)}{\partial h^2}. \tag{18}$$

Since $h \propto m_\pi^2$ is proportional to the bare quark mass, the above definition gives a susceptibility which is proportional to the usual definition around the critical point, $\chi_\sigma = -\partial^2\Omega/\partial M^2/T^2$, where M is the bare quark mass. We normalize Eqs. (18) by multiplying some powers of T to consider dimensionless susceptibility. Figure 3 shows the chiral susceptibility as a function of temperature for several baryon chemical potentials at $\delta\mu = 0$ MeV. For each μ_B, we find a peak in χ_σ, where the chiral phase transition occurs. At CP, $(T, \mu_B) = (T_{\rm CP}, \mu_{\rm CP})$, this quantity is divergent which signals a second-order phase transition. The critical points are found to be $(T_{\rm CP}, \mu_{\rm CP}) = (117, 975)$ MeV at $\delta\mu = 0$ without vector coupling $r = 0$.

As in the case of the chiral transition, the deconfinement transition is a crossover for finite quark masses, and we need to specify a criterion to identify the deconfinement

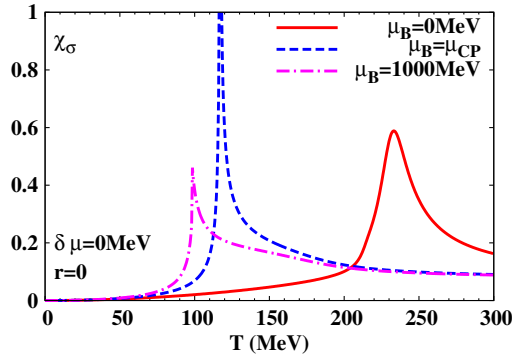

FIG. 3 (color online). The chiral susceptibility χ_σ as a function of temperature for different isospin chemical potentials $\mu_B = 0$ (solid line), $\mu_{\rm CP}$ (dash line), 1000 MeV (dash-dot line) at $\delta\mu = 0$ MeV. χ_σ is divergent at the critical end point.

phase boundary. Several prescriptions to define the critical temperature for deconfinement have been used in the literature: the temperature at which the Polyakov loop susceptibility, χ_P, is maximum; the temperature at which dP/dT is maximum [29,30]; and, finally, the half-value prescription, in which one identifies the deconfinement temperature with the average of the temperatures at which at $P = 1/2$ and $\bar{P} = 1/2$ [31] (the two differ at finite μ). The Polyakov loop susceptibility is defined as $\chi_P \equiv -T^2\partial^2\Omega/\partial\eta\partial\bar{\eta}|_{\eta,\bar{\eta}=0}$, where η and $\bar{\eta}$ are the Polyakov loop source inserted in the potential as $\Omega \to \Omega - T(\eta P + \bar{\eta}\,\bar{P})$ [32]. It may have a double peak structure in some cases [13]: one peak is related to the chiral phase transition and the other is related to the transition caused by the Polyakov loop mean-field potential. A similar double peak behavior is found in dP/dT [29,30]. Thus, it is not easy to unambiguously define the deconfinement temperature from the Polyakov loop susceptibility or the temperature derivative. Since the Polyakov loop is small (P, $\bar{P} \simeq 0$) in confined phase and large (P, $\bar{P} \simeq 1$) in deconfined phase, the half-value prescription is the simplest one to adopt. Figure 4 shows the confinement-deconfinement phase boundaries defined by the peaks of dP/dT and χ_P and in the half-value prescription. These boundaries are qualitatively the same, but there are two differences. First, the phase boundaries defined by the peaks of dP/dT and χ_P have a cusp because of the double peak structure in dP/dT and χ_P. At $\mu_B \gtrsim 800$ MeV, we clearly find two peaks and the lower peak temperature corresponds to the chiral transition. Thus the higher peak temperature is assigned as the deconfinement temperature. The phase boundary defined in the half-value prescription is smooth. Secondly, the transition temperature defined in the half-value prescription is about 30 MeV higher than those defined by the others. Since we focus our attention on the first-order phase boundary and CP, these differences in the deconfinement transition temperatures do not change our conclusions. Thus, we show the deconfinement transition temperature in the half-value prescription in the later discussion for simplicity.

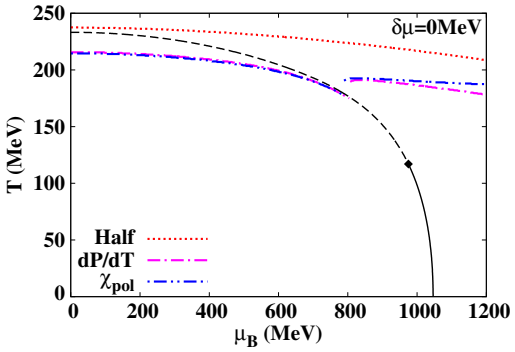

FIG. 4 (color online). The confinement-deconfinement phase boundaries defined by three prescriptions: peaks of dP/dT (dot-dot-dashed line) and χ_P (dot-dashed line) and the half-value prescription (dotted line). The dashed and solid lines show the crossover and first-order chiral phase boundaries.

We show the QCD phase boundaries for several $\delta\mu$ values in Fig. 5. The hadron phase shrinks a little and the critical point temperature $T_{\rm CP}$ decreases with increasing $\delta\mu$, while the confinement-deconfinement phase boundary only weakly depends on $\delta\mu$. The reduction of the transition chemical potential may be understood as the density effects. For a simple estimate, let us consider the low-T transition in the chiral limit without the vector coupling, where the sum of u and d quark number densities in the chiral restored phase is proportional to $(\mu + \delta\mu)^3 + (\mu - \delta\mu)^3 = 2\mu^3(1 + 3\delta\mu^2/\mu^2)$ as in the free massless case. If the QCD phase transition at finite $\delta\mu$ occurs at the same density in the Wigner phase as that for $\delta\mu = 0$, the transition quark chemical potential is calculated to be $\mu \simeq \mu_c - \delta\mu^2/\mu_c$, where μ_c represents the transition chemical potential at $\delta\mu = 0$. This estimate gives the transition chemical potential shifts of 7.2 and 14 MeV for $\delta\mu = 50$ and 70 MeV, respectively, which is comparable to the PQM results, 7.0 and 13 MeV. Another possible explanation is the decrease of the effective number of flavors. At finite $\delta\mu$, one of the u or d quarks is favored, and the phase diagram is expected to be closer to that at $N_f = 1$, where the phase transition is weaker.

We note that the deconfinement transition temperature T_d in the half-value prescription is a little higher than the chiral transition temperature T_c. This order is the same as the lattice Monte Carlo simulation results, which suggest $T_d > T_c$ [33]. It should be noted, however, that T_d in the lattice results is defined as the peak position of dP/dT (inflection point). T_d defined by the peak of dP/dT is smaller than T_c in the present parametrization and in the previous work [34]. While the order of T_d and T_c at $\mu = 0$ is an interesting problem on the relation of deconfinement and chiral transitions, it is irrelevant to our conclusion, and we choose $T_0 = 270$ MeV in the later discussion.

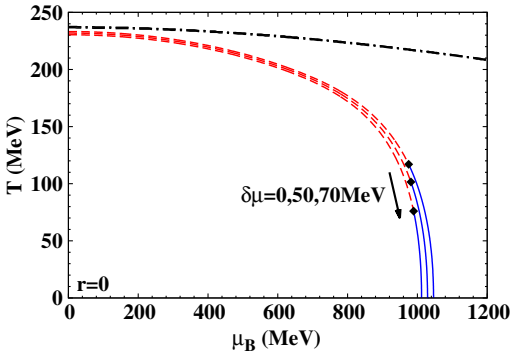

FIG. 5 (color online). The QCD phase diagrams for several isospin chemical potentials. The red dash and the blue solid lines show the crossover and first-order chiral phase transition boundaries, respectively, at $\delta\mu = 0$, 50, 70 MeV. The square dots show the CP. The black dot-dashed lines show the confinement-deconfinement phase boundaries at $\delta\mu = 0$, 70 MeV.

It should be noted that the deconfinement phase boundary is almost insensitive to the baryon chemical potential, leading to a splitting of the chiral and deconfinement transition boundaries. This behavior is similar to the strong coupling lattice QCD results including finite coupling and Polyakov loop effects [30], but it is different from the results obtained from the functional renormalization group method starting from the PQM initial condition at large cutoff [35].

Figure 6 shows the QCD phase diagrams of symmetric matter ($\delta\mu = 0$) for several quark-vector meson couplings. With increasing vector coupling, the chiral phase boundary moves to the higher μ_B direction, and the CP moves to the higher-μ_B and lower-T direction. The behavior of $\mu_{\rm CP}$ is understood from the effective μ_B shift. We can ignore the ρ^0 meson effects in symmetric matter, and the effective chemical potential is given as $\tilde{\mu} = \mu - rg\omega$. Therefore, a strong vector interaction makes $\tilde{\mu}$ small for a given μ_B [32], and the phase boundaries and the CP move to high μ_B for finite vector coupling, $r \neq 0$. By comparison, the vector coupling dependence of the confinement-deconfinement phase boundary is small.

We show the QCD phase diagram in $(T, \mu_B, \delta\mu)$ space in Fig. 7. As already mentioned, $\delta\mu$ reduces $T_{\rm CP}$ and the transition baryon chemical potential at $T = 0$. Then the first-order boundary narrows with increasing $\delta\mu$, and eventually the CP disappears at a certain value of $\delta\mu$. This happens also for the NJL model, as we discuss in more detail in the Appendix. This behavior is important when we consider the chiral phase transition in dense and isospin asymmetric matter, which is realized in the core of neutron stars, where $\delta\mu$ becomes large. For example, the reduced CP temperature may affect the dynamical BH formation processes. The highest temperature during the BH formation is calculated to be $T \sim 70$ MeV, and compressed matter may experience either the first-order, crossover, or CP sweep depending on the CP location in asymmetric matter [6].

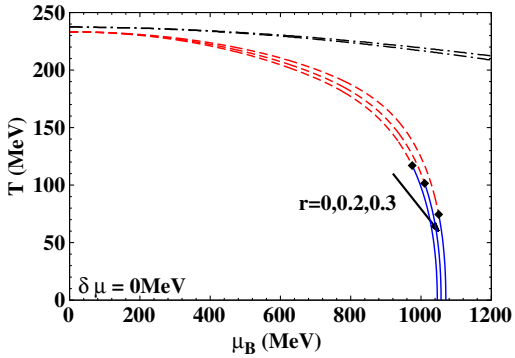

FIG. 6 (color online). The QCD phase diagrams for several quark-vector meson couplings. The red dash and blue solid lines show the crossover and first-order chiral phase transition boundaries, respectively, at $r = 0$, 0.2, 0.3. The black dot-dashed lines show the confinement-deconfinement phase boundaries at $r = 0$ and $r = 0.2$.

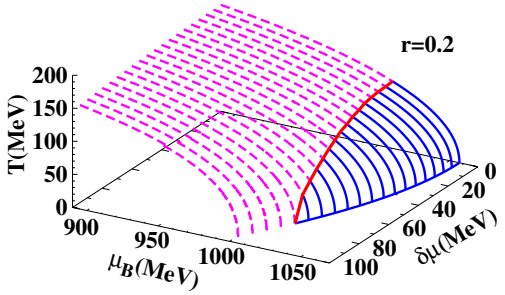

FIG. 7 (color online). The three-dimensional $(T, \mu_B, \delta\mu)$ QCD phase diagram in PQM with $r = 0.2$. The dash lines and the blue solid lines show the crossover and first-order chiral phase boundary, respectively. The red solid line shows CP for different $\delta\mu$.

B. Phase transition in neutron star matter

Another example of dense asymmetric matter is the neutron star core. In the neutron star core, the internal temperature is of the order of 10^6 K $\sim 10^{-4}$ MeV, which is small enough compared with the Fermi energy of neutrons. The baryon density would reach a few times of the nuclear density, $\sim 10^{15}$ g/cm^3. Since the neutron density is much larger than the proton density, the isospin chemical potential, $\delta\mu = (\mu_n - \mu_p)/2 = (\mu_d - \mu_u)/2$, is finite and large. In relativistic mean-field (RMF) models, $\delta\mu$ is calculated to reach 100 MeV in the neutron star core. Thus, we can regard the neutron star core matter as asymmetric matter at zero temperature.

In Fig. 8, we compare the β equilibrium line at $T = 0$ in PQM with the first-order phase transition boundary. Here we show the boundaries for several values of r, $r = 0$, 0.2, 0.3, and 0.37. The β equilibrium line corresponds to neutron star matter; the charge-neutral condition at $T = 0$ is solved under the neutrinoless β equilibrium condition,

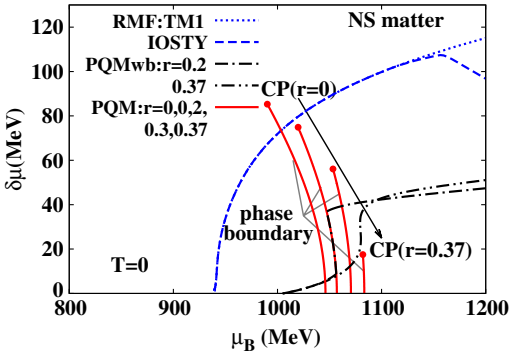

FIG. 8 (color online). Comparison of the first-order phase transition boundaries and the β equilibrium lines. Solid lines show the first-order phase boundaries in PQM at $T = 0$ with $r = 0$, 0.2, 0.3, and 0.37. Dot-dashed and dot-dot-dashed lines show the β equilibrium lines $(\mu_B, \delta\mu)$ for neutron star matter calculated in PQM with $r = 0.2$ and 0.37, respectively. The β equilibrium lines in hadronic EOS are shown for TM1 [37] (dotted line) and IOSTY [38] (dashed line).

$\delta\mu = \mu_e/2$. The phase transition in neutron star matter is calculated to be the first order, when the vector coupling is small, $r \lesssim 0.36$. Similar results are obtained in the flavor SU(3) NJL model [36]. At large vector coupling $r \gtrsim 0.37$, the chiral phase transition in neutron star becomes crossover; the β equilibrium line is above the first-order phase transition boundary in the $(\mu_B, \delta\mu)$ plane. For $r \gtrsim 0.38$, large vector coupling makes the chiral transition crossover even at $\delta\mu = 0$.

In Fig. 8, we also show the β equilibrium line in RMF at $T = 0$ [25]. RMF parameter sets of TM1 [37] and IOSTY [38] are adopted as typical examples. TM1 is a model that describes bulk properties of normal and neutron-rich nuclei as well as the nuclear matter saturation point. IOSTY is an extended version of TM1, which includes degrees of freedom of nucleons and hyperons. RMF predicts large $\delta\mu$ values, $\delta\mu \sim 100$ MeV, in neutron star core, and the β equilibrium line is above the first-order transition boundaries in PQM for $r = 0.2$, 0.3 and 0.37. In IOSTY, hyperons are calculated to appear at $\mu_B \simeq 1100$ MeV, then the transition to quark matter occurs before hyperons appear.

The PQM results of $\delta\mu$ in neutron star matter are much smaller than those in RMF. The difference of $\delta\mu$ values in PQM and RMF mainly comes from the isovector coupling with quarks and nucleons. In quark matter, we have chosen the vector coupling in the range $0 \leq r \leq 0.37$. In nuclear matter, isovector-vector coupling is chosen to reproduce binding energies of neutron-rich nuclei, and it corresponds to $r \simeq 1.0$–1.2. The isovector-vector potential shifts $\delta\mu$, and $\delta\mu$ is calculated to be large in nuclear matter.

The RMF results of $\delta\mu$ are based on properties of neutron-rich nuclei observed in laboratory experiments, and they should be more reliable than the PQM results at low densities. Therefore, the comparison of the β equilibrium line in RMF and the first-order phase boundaries suggests that the phase transition in neutron star matter would be crossover. Since the first-order transition generally makes the equation of state softer at around the transition density, the crossover nature may help to keep the EOS stiff enough and to support the heavy neutron stars [39].

IV. SUMMARY

We have investigated the QCD phase transition in isospin asymmetric matter using the Polyakov loop extended quark meson (PQM) model. Specifically, we have discussed isospin chemical potential $\delta\mu$ and quark-vector meson coupling dependence of the QCD phase boundaries. In PQM, we show $\delta\mu$ reduces the temperature of the QCD critical point (CP), and for large $\delta\mu$, the CP is found to disappear. We also show the finite quark-vector meson coupling shifts the chiral phase boundary to higher baryon chemical potential and reduces the temperature of the CP. This scenario is in agreement with the one obtained in other chiral models [6,36].

We have also discussed the order of the chiral phase transition in neutron star matter from the comparison of the QCD phase diagram in PQM and the β equilibrium line. In RMF, $\delta\mu$ is found to be large enough for the CP to disappear for moderate values of the vector coupling, $r \equiv g_v/g \gtrsim 0.2$. Then the chiral phase transition may be crossover, even if the transition in symmetric matter ($\delta\mu = 0$) is the first order. It should be noted, however, that the phase transition in neutron star matter is calculated to be the first order for $r \lesssim 0.37$ in PQM. In order to more seriously discuss the QCD phase transition in compact astrophysical phenomena, we need the EOS that includes both baryonic and quark degrees of freedom.

One may consider that the reduction of $T_{\rm CP}$ shown in this paper would contradict the finite lepton-number chemical potential result in [24], which suggests the insensitivity of $T_{\rm CP}$ as a function of the lepton-number chemical potential. Their results correspond to the $\delta\mu$ range $\delta\mu \lesssim 40$ MeV, while we find that the shift of $T_{\rm CP}$ is large in the range $\delta\mu \gtrsim 50$ MeV. Thus, their results could be consistent with ours.

The phase diagram structure shown in this paper is based on the assumption that the s-wave pion condensation is not realized in neutron star matter following the s-wave πN repulsion arguments [25] and the functional renormalization group calculation [23]. If the s-wave pion-condensed phase is connected with the first-order chiral transition boundary, the phase diagram in $(T, \mu_B, \delta\mu)$ space may have a more complex structure as shown in the mean-field treatment of PNJL [22].

In a future work, it would be interesting to discuss the p-wave pion condensation, the inhomogeneous chiral condensate, and the color superconductor phases in the three-dimensional thermodynamic variable space $(T, \mu, \delta\mu)$.

ACKNOWLEDGMENTS

T. N. and H. U. are supported by Grants-in-Aid for the Japan Society for Promotion of Science(JSPS) Research Fellows (No. 22-3314 and No. 25-2148). This work was supported in part by Grants-in-Aid for Scientific Research from the Japan Society for the Promotion of Science (JSPS) (No. 23340067, No. 24340054, and No. 24540271 10J03314), by a Grant-in-Aid for Innovative Areas from the Ministry of Education, Culture, Sports, Science and Technology of Japan (MEXT) (Area No. 2404, No. 24105001, No. 24105008), by the Yukawa International Program for Quark-Hadron Sciences, and by a Grant-in-Aid for the global COE program "The Next Generation of Physics, Spun from Universality and Emergence" from MEXT.

APPENDIX: CRITICAL POINT WITHIN THE NJL MODEL AT ZERO TEMPERATURE

In the main body of this paper we have discussed the effect of an imbalance of the chemical potentials of u and d

quarks on the location of the critical point (CP) of the QCD phase diagram. Our argument was based mainly on numerical results obtained within the PQM model. We found that finite $\delta\mu$ moves CP towards a smaller chemical potential and a lower temperature. Therefore, we might expect that a large-enough $\delta\mu$ causes CP to hit the $T = 0$ plane, then disappear from the phase diagram. In this Appendix we discuss the same topic within the NJL model. We limit ourselves to consider a system of u and d quarks in the chiral limit: this simplifies the calculations and allows us to identify unambiguously the location of the chiral phase transition in the phase diagram. Our purpose is to show analytically how finite $\delta\mu$ induces a softening of the chiral phase transition at finite μ, pushing the CP to lower values of temperature (and baryon chemical potential). Eventually, for large-enough $\delta\mu$, the CP hits the $T = 0$ plane. For the purpose of our discussion, it is therefore enough to consider the system at $T = 0$ and study the change of the order of the chiral phase transition at finite μ.

The thermodynamic potential of the NJL model at zero temperature can be written as [10]

$$\Omega = \frac{\sigma^2}{G} - 2N_c N_f \int \frac{d\boldsymbol{p}}{(2\pi)^3} E_p + 2N_c \sum_f \int \frac{d\boldsymbol{p}}{(2\pi)^3} (E_p - \mu_f)\Theta(\mu_f - E_p), \quad \text{(A1)}$$

where $E_p = \sqrt{\boldsymbol{p}^2 + M^2}$ with $M = 2\sigma = -4G\langle\bar{q}_f q_f\rangle$. Here, G corresponds to the 4-fermion NJL coupling constant, and in agreement with the notation of the main text, we have put $\mu_u = \mu - \delta\mu$ and $\mu_d = \mu + \delta\mu$. The last addendum on the rhs of the above equation corresponds to the valence quarks' contributions. The vacuum part is regularized by cutting the momentum integral at the scale $|\boldsymbol{p}| = \Lambda$.

Our strategy is as follows: we perform a Ginzburg-Landau expansion of the effective potential,

$$\Omega = \frac{\alpha_2}{2}\sigma^2 + \frac{\alpha_4}{4}\sigma^4 + \frac{\alpha_6}{6}\sigma^6, \quad \text{(A2)}$$

where we have subtracted an irrelevant term that does not depend on the condensate. At zero temperature and finite chemical potential, the coefficients are easily determined from an expansion of Eq. (A1) around $\sigma = 0$. We get

$$\alpha_2 = \frac{2}{G} - \frac{4N_c}{\pi^2}\Lambda^2 + \frac{2N_c}{\pi^2}(\mu_u^2 + \mu_d^2), \quad \text{(A3)}$$

$$\alpha_4 = -\frac{48N_c}{\pi^2}\left(2 - \log\frac{\Lambda^2}{\mu_u\mu_d}\right), \quad \text{(A4)}$$

$$\alpha_6 = \frac{480N_c}{\pi^2}\left(\frac{1}{\mu_u^2} + \frac{1}{\mu_d^2}\right). \quad \text{(A5)}$$

We notice that $\alpha_6 > 0$, causing the potential to be bounded from below. As a consequence it is possible to study the phase transition studying the signs of the first two coefficients. The phase transition is of first (second) order if $\alpha_4 < 0$ ($\alpha_4 > 0$). At the critical point, where the first- and second-order transition lines meet, one has $\alpha_2 = \alpha_4 = 0$. Solving $\alpha_2 = 0$ leads to a relationship between μ and $\delta\mu$; using the solution of the latter in the equation $\alpha_4 = 0$ leads to the critical value of $\delta\mu \equiv \delta\mu_c$ at which the CP hits the $T = 0$ plane, namely,

$$\delta\mu_c^2 = -\frac{\pi^2}{2GN_cN_f} + \Lambda^2\left(\frac{1 - e^{-2}}{2}\right). \quad \text{(A6)}$$

Using the standard parameters of the model [10], we find $\delta\mu_c \approx 140$ MeV. This result shows that finite $\delta\mu$ changes the order of the chiral phase transition at zero temperature and finite chemical potential.

The fact that finite $\delta\mu$ leads to the softening of the phase transition can be grasped from Eq. (A4); in fact, for $\delta\mu \ll \mu$ one has

$$\alpha_4 \approx \alpha_4(\delta\mu = 0) + \frac{48N_c}{\pi^2}\frac{\delta\mu^2}{\mu^2}; \quad \text{(A7)}$$

the above equation shows that $\delta\mu \neq 0$ makes α_4 less negative, thus favoring a second-order phase transition. The same conclusion can be drawn by using an extended version of the Ginzburg-Landau analysis, including derivative terms [40].

[1] See, for example, P. Haensel, A. Y. Potekhin, and D. G. Yakovlev, *Neutron Stars 1: Equation of State and Structure*, Astrophysics and space science library Vol. 326 (Springer Science+Business Media, LLC, New York, 2007).

[2] T. Hatsuda, Mod. Phys. Lett. A **02**, 805 (1987); I. Sagert, T. Fischer, M. Hempel, G. Pagliara, J. Schaffner-Bielich, A. Mezzacappa, F.-K. Thielemann, and M. Liebendörfer, Phys. Rev. Lett. **102**, 081101 (2009).

[3] K. Sumiyoshi, S. Yamada, H. Suzuki, and S. Chiba, Phys. Rev. Lett. **97**, 091101 (2006).

[4] K. Sumiyoshi, S. Yamada, and H. Suzuki, Astrophys. J. **667**, 382 (2007).

[5] K. Sumiyoshi, C. Ishizuka, A. Ohnishi, S. Yamada, and H. Suzuki, Astrophys. J. Lett. **690**, L43 (2009).

[6] A. Ohnishi, H. Ueda, T. Z. Nakano, M. Ruggieri, and K. Sumiyoshi, Phys. Lett. B **704**, 284 (2011).

[7] F. Karsch, Lect. Notes Phys. **583**, 209 (2002).

[8] J. Greensite, Prog. Part. Nucl. Phys. **51**, 1 (2003).

[9] Z. Fodor and S. D. Katz, J. High Energy Phys. 03 (2002) 014; S. Ejiri, C. R. Allton, S. J. Hands, O. Kaczmarek, F. Karsch, E. Laermann, and C. Schmidt, Prog. Theor. Phys. Suppl. **153**, 118 (2004); R. V. Gavai and S. Gupta, Phys. Rev. D **71**, 114014 (2005); P. de Forcrand, S. Kim, and O. Philipsen, Proc. Sci., LAT (2007) 178; P. de Forcrand and O. Philipsen, J. High Energy Phys. 11 (2008) 012.

[10] Y. Nambu and G. Jona-Lasinio, Phys. Rev. **122**, 345 (1961); **124**, 246 (1961); U. Vogl and W. Weise, Prog. Part. Nucl. Phys. **27**, 195 (1991); S. P. Klevansky, Rev. Mod. Phys. **64**, 649 (1992); T. Hatsuda and T. Kunihiro, Phys. Rep. **247**, 221 (1994); M. Buballa, Phys. Rep. **407**, 205 (2005).

[11] D. U. Jungnickel and C. Wetterich, Phys. Rev. D **53**, 5142 (1996).

[12] P. N. Meisinger and M. C. Ogilvie, Phys. Lett. B **379**, 163 (1996).

[13] K. Fukushima, Phys. Lett. B **591**, 277 (2004).

[14] C. Ratti, M. A. Thaler, and W. Weise, Phys. Rev. D **73**, 014019 (2006); S. Rossner, C. Ratti, and W. Weise, Phys. Rev. D **75**, 034007 (2007); C. Sasaki, B. Friman, and K. Redlich, Phys. Rev. D **75**, 074013 (2007).

[15] B. J. Schaefer, J. M. Pawlowski, and J. Wambach, Phys. Rev. D **76**, 074023 (2007).

[16] V. Skokov, B. Friman, E. Nakano, K. Redlich, and B. J. Schaefer, Phys. Rev. D **82**, 034029 (2010).

[17] M. A. Stephanov, Proc. Sci., LAT (2006) 024.

[18] B. Mohanty (STAR Collaboration), J. Phys. G **38**, 124023 (2011); J. T. Mitchell (PHENIX Collaboration), Nucl. Phys. **A904–905**, 903c (2013).

[19] M. A. Stephanov, K. Rajagopal, and E. V. Shuryak, Phys. Rev. Lett. **81**, 4816 (1998); D. T. Son and M. A. Stephanov, Phys. Rev. D **70**, 056001 (2004); H. Fujii, Phys. Rev. D **67**, 094018 (2003); M. A. Stephanov, Phys. Rev. Lett. **102**, 032301 (2009); Y. Minami and T. Kunihiro, Prog. Theor. Phys. **122**, 881 (2009); M. A. Stephanov, K. Rajagopal, and E. V. Shuryak, Phys. Rev. D **60**, 114028 (1999).

[20] R. Oechslin and H.-T. Janka, Phys. Rev. Lett. **99**, 121102 (2007); L. Baiotti, B. Giacomazzo, and L. Rezzolla, Phys. Rev. D **78**, 084033 (2008); K. Kiuchi, Y. Sekiguchi, M. Shibata, and K. Taniguchi, Phys. Rev. Lett. **104**, 141101 (2010); K. Hotokezaka, K. Kyutoku, H. Okawa, M. Shibata, and K. Kiuchi, Phys. Rev. D **83**, 124008 (2011).

[21] H. Abuki, M. Ciminale, R. Gatto, N. D. Ippolito, G. Nardulli, and M. Ruggieri, Phys. Rev. D **78**, 014002 (2008); H. Abuki, R. Anglani, R. Gatto, G. Nardulli, and M. Ruggieri, Phys. Rev. D **78**, 034034 (2008);

[22] T. Sasaki, Y. Sakai, H. Kouno, and M. Yahiro, Phys. Rev. D **82**, 116004 (2010); J. O. Andersen and L. Kyllingstad, J. Phys. G **37**, 015003 (2010).

[23] K. Kamikado, N. Strodthoff, L. von Smekal, and J. Wambach, Phys. Lett. B **718**, 1044 (2013).

[24] S. B. Ruster, V. Werth, M. Buballa, I. A. Shovkovy, and D. H. Rischke, Phys. Rev. D **73**, 034025 (2006).

[25] A. Ohnishi, D. Jido, T. Sekihara, and K. Tsubakihara, Phys. Rev. C **80**, 038202 (2009).

[26] M. Kitazawa, T. Koide, T. Kunihiro, and Y. Nemoto, Nucl. Phys. **A721**, C289 (2003); Z. Zhang and T. Kunihiro, Phys. Rev. D **80**, 014015 (2009); O. Lourenco, M. Dutra, T. Frederico, A. Delfino, and M. Malheiro, Phys. Rev. D **85**, 097504 (2012).

[27] G. Boyd, J. Engels, F. Karsch, E. Laermann, C. Legeland, M. Lutgemeier, and B. Petersson, Nucl. Phys. **B469**, 419 (1996).

[28] K. Fukushima, Phys. Lett. B **695**, 387 (2011).

[29] T. Kahara and K. Tuominen, Phys. Rev. D **78**, 034015 (2008).

[30] K. Miura, T. Z. Nakano, A. Ohnishi, and N. Kawamoto, arXiv:1106.1219; T. Z. Nakano, K. Miura, and A. Ohnishi, Phys. Rev. D **83**, 016014 (2011).

[31] T. Kahara and K. Tuominen, Phys. Rev. D **82**, 114026 (2010).

[32] K. Fukushima, Phys. Rev. D **77**, 114028 (2008); **78**, 039902(E) (2008).

[33] Y. Aoki, Z. Fodor, S. D. Katz, and K. K. Szabo, Phys. Lett. B **643**, 46 (2006); S. Ejiri, Y. Maezawa, N. Ukita, S. Aoki, T. Hatsuda, N. Ishii, K. Kanaya, and T. Umeda (WHOT-QCD Collaboration), Phys. Rev. D **82**, 014508 (2010); M. Cheng, N. H. Christ, M. Li, R. D. Mawhinney, D. Renfrew, P. Hegde, F. Karsch, M. Lin, and P. Vranas, Phys. Rev. D **81**, 054510 (2010); A. Bazavov, and P. Petreczky (HotQCD Collaboration), J. Phys. G **38**, 124099 (2011).

[34] B.-J. Schaefer, M. Wagner, and J. Wambach, Phys. Rev. D **81**, 074013 (2010).

[35] B.-J. Schaefer, J. M. Pawlowski, and J. Wambach, Phys. Rev. D **76**, 074023 (2007); T. K. Herbst, J. M. Pawlowski, and B.-J. Schaefer, Phys. Lett. B **696**, 58 (2011).

[36] H. Abuki, R. Gatto, and M. Ruggieri, Phys. Rev. D **80**, 074019 (2009).

[37] Y. Sugahara and H. Toki, Nucl. Phys. **A579**, 557 (1994).

[38] C. Ishizuka, A. Ohnishi, K. Tsubakihara, K. Sumiyoshi, and S. Yamada, J. Phys. G G **35**, 085201 (2008).

[39] P. Demorest, T. Pennucci, S. Ransom, M. Roberts, and J. Hessels, Nature (London) **467**, 1081 (2010).

[40] Y. Iwata, H. Abuki, and K. Suzuki, AIP Conf. Proc. **1492**, 293 (2012); H. Abuki, Phys. Rev. D **87**, 094006 (2013).